

---

# Evaluation of 5-<sup>11</sup>C-Methyl-A-85380 as an Imaging Agent for PET Investigations of Brain Nicotinic Acetylcholine Receptors

Yasuhiko Iida, PhD<sup>1</sup>; Mikako Ogawa, MS<sup>2</sup>; Masashi Ueda, MS<sup>1</sup>; Akiko Tominaga, MS<sup>1</sup>; Hidekazu Kawashima, PhD<sup>1</sup>; Yasuhiro Magata, PhD<sup>2</sup>; Shingo Nishiyama, MS<sup>3</sup>; Hideo Tsukada, PhD<sup>3</sup>; Takahiro Mukai, PhD<sup>4</sup>; and Hideo Saji, PhD<sup>1</sup>

<sup>1</sup>Department of Patho-Functional Bioanalysis, Graduate School of Pharmaceutical Sciences, Kyoto University, Kyoto, Japan;

<sup>2</sup>Laboratory of Genome Bio-Photonics, Photon Medical Research Center, Hamamatsu University School of Medicine,

Hamamatsu, Japan; <sup>3</sup>Central Research Laboratory, Hamamatsu Photonics K.K., Hamamatsu, Japan; and <sup>4</sup>Department of

Nuclear Medicine, Graduate School of Medicine, Kyoto University, Japan

---

Central nicotinic acetylcholine receptors (nAChRs) represent major neurotransmitter receptors responsible for various brain functions, and changes in the density of nAChRs have recently been reported in several neurodegenerative diseases. Visualization of nAChRs in human brain has thus been of great interest, and the development of radiopharmaceuticals for the imaging and quantitative assessment of central nAChRs has been desired. In this study, we synthesized 5-<sup>11</sup>C-methyl-3-(2-(S)-azetidylmethoxy)pyridine (5MA), a derivative of 3-(2-(S)-azetidylmethoxy)pyridine (A-85380) <sup>11</sup>C-methylated at position 5 of the pyridyl fragment, and evaluated its potential for investigating central nAChRs by PET. **Methods:** <sup>11</sup>C-5MA was synthesized by the incorporation of <sup>11</sup>C-methyl iodide into 5-butylstannyl A-85380, using a Pd-catalyzed coupling reaction. The affinity of 5MA for central nAChRs was measured by displacement of (–)-<sup>3</sup>H-cytisine from binding sites in rat cortical membranes. The biodistribution of <sup>11</sup>C-5MA was determined with mice. PET studies were performed on rhesus monkeys with a high-resolution PET scanner for animals. **Results:** The overall synthesis time was 60 min from the end of radionuclide production, and the radiochemical yield, after purification by high-performance liquid chromatography, was 30%. The radiochemical purity of the product was >99%, with a specific radioactivity of >36 GBq/μmol. In vitro receptor-binding assays demonstrated that 5MA has a high, selective binding affinity for nAChRs, being approximately 1.5-fold higher than that of A-85380, 3.5-fold higher than that of (–)-cytisine, and 10-fold higher than that of (–)-nicotine. The distribution studies in mice showed that the brain uptake of <sup>11</sup>C-5MA was profound. Regional cerebral distribution studies in mice demonstrated that the accumulation of <sup>11</sup>C-5MA was consistent with the density of nAChRs, with the highest uptake observed in the thalamus, a moderate uptake in the cortex and striatum, and the lowest uptake in the cerebellum. Furthermore, preinjection of nAChR-binding ligands, (–)-nicotine and (–)-cytisine, reduced the uptake of <sup>11</sup>C-5MA in brain regions of high uptake in the untreated experiment. PET imaging studies with <sup>11</sup>C-5MA in rhesus monkeys demonstrated

clear images consistent with the distribution of nAChRs in the brain. **Conclusion:** These results suggest that <sup>11</sup>C-5MA is a potential PET radiopharmaceutical for nuclear medical studies of nAChRs in the brain.

**Key Words:** central nicotinic acetylcholine receptors; 5-<sup>11</sup>C-methyl-3-(2-(S)-azetidylmethoxy)pyridine; receptor-binding affinity; biodistribution; PET

**J Nucl Med 2004; 45:878–884**

---

Nicotinic acetylcholine receptors (nAChRs) have been implicated in a variety of brain functions and behavioral states, including learning, memory, attention, and anxiety (1–4). Furthermore, a decrease in central nAChRs has been observed in several neurodegenerative diseases, including Alzheimer's disease (5–8) and Parkinson's disease (9,10). In addition, increases in nAChRs have been observed in the brains of smokers (11).

Thus, imaging for nAChRs in the brain with PET or SPECT has been of great interest for the evaluation of brain functions and diagnosis of neurodegenerative diseases. For this purpose, several radiotracers for PET or SPECT of nAChRs have been developed (12–16). Among these compounds, <sup>18</sup>F-fluorinated and <sup>125</sup>I-iodinated derivatives of 3-(2-(S)-azetidylmethoxy)pyridine (A-85380) are promising because of their high, selective affinity for α<sub>4</sub>β<sub>2</sub>, the predominant subtype of nAChR in the brain, high cerebral accumulation, and low toxicity (12,17–27).

5-Methyl-3-(2-(S)-azetidylmethoxy)pyridine (5MA), an A-85380 derivative methylated at position 5 of the pyridyl fragment, has recently been reported to have high affinity for nAChRs (28). In this study, <sup>11</sup>C-5MA was synthesized and its receptor-binding affinity, biodistribution in rodents, and imaging with PET in rhesus monkeys were investigated to evaluate its potential for investigating central nAChRs by PET.

---

Received Oct. 7, 2003; revision accepted Dec. 29, 2003.

For correspondence or reprints contact: Hideo Saji, PhD, Department of Patho-Functional Bioanalysis, Graduate School of Pharmaceutical Sciences, Kyoto University, Sakyo-ku, Kyoto 606-8501, Japan.

E-mail: hsaji@pharm.kyoto-u.ac.jp

## MATERIALS AND METHODS

(-)-<sup>3</sup>H-Cytisine (1.48 TBq/mmol) was purchased from NEN Life Science Products, Inc. Nonradioactive 5MA was synthesized according to the method of Karimi and Langstrom (29), and its structure was confirmed by proton nuclear magnetic resonance, mass spectrometry, and elemental analyses. All other chemicals used were of reagent grade. Male ddY mice and Wistar rats were supplied by Japan SLC Co. Ltd. and male rhesus monkeys (*Macaca mulatta*) were obtained from Clea Japan, Inc. The animal studies were conducted according to guidelines stipulated by the Kyoto University Animal Care and Use Committee.

### Radiosynthesis of <sup>11</sup>C-5MA

<sup>11</sup>C was produced via a <sup>14</sup>N(p, α)<sup>11</sup>C reaction with 11.3-MeV protons on a target of nitrogen gas by an ultracompact cyclotron (CYPRIS model 325; Sumitomo Heavy Industry Ltd.). The <sup>11</sup>CO<sub>2</sub> produced was transported to an automated synthesis system of <sup>11</sup>C-methyl iodide (CUPID C-100; Sumitomo Heavy Industry Ltd.). The synthesis of <sup>11</sup>C-5MA is outlined in Figure 1. A precursor, 5-(tri-*n*-butylstannyl)-3-((*S*)-1-(*tert*-butoxycarbonyl)-2-azetidinylmethoxy)pyridine, was prepared according to methods described in the literature (21,25,27). The precursor (1 mg) was dissolved in 0.5 mL of freshly distilled *N,N*-dimethylformamide and added into the reaction vessel containing tris(dibenzylideneacetone)dipalladium (4.6 mg), tri-*o*-tolylphosphine (6.1 mg), CuCl (2.0 mg), and K<sub>2</sub>CO<sub>3</sub> (2.8 mg) under argon gas. The <sup>11</sup>C-methyl iodide synthesized was transferred to the reaction vessel via a nitrogen stream. After heating at 80°C for 3 min, the vessel was cooled with chilled air. Cleavage of the *tert*-butoxycarbonyl protection was achieved by adding 1.0 mL of trifluoroacetic acid and heating at 100°C for 5 min. After neutralization with the 6N NaOH solution, the reaction solution was diluted with 10 mL of water and loaded on an OASIS column (Waters). After the column was washed with 2 mL of aqueous 5% methanol solution, radioactivity was eluted with 0.5 mL of methanol. The eluted methanol solution was then applied to a preparative high-performance liquid chromatography column (COSMOSIL 5C18-AR-300, 10 × 250 mm; Nakalai), and <sup>11</sup>C-5MA was eluted with 0.6% triethylamine in acetonitrile and 0.01 mol/L ammonium acetate (3:1) at a flow rate 3.5 mL/min (retention time = 12 min for <sup>11</sup>C-5MA). After collection of the radioactivity of <sup>11</sup>C-5MA, the organic solvent was removed in vacuo. The residue was diluted with saline and filtered through a sterile 0.2-μm membrane filter into a sterile vial.

### In Vitro nAChR-Binding Studies

The affinity of 5MA for nAChRs was measured on the basis of the displacement of (-)-<sup>3</sup>H-cytisine from a preparation of rat cerebral cortical synaptosomal membranes, according to the

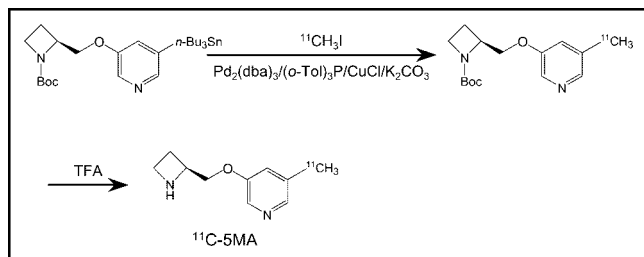


**FIGURE 1.** Radiosynthesis of <sup>11</sup>C-5MA. TFA = trifluoroacetic acid.

method of Pabreza et al. (30) with a slight modification. In brief, the cerebral cortex of male Wistar rats (230–250 g) was homogenized in 50 mmol/L Tris-HCl buffer (pH 7.4) containing 120 mmol/L NaCl, 5 mmol/L KCl, 1 mmol/L MgCl<sub>2</sub>, and 2.5 mmol/L CaCl<sub>2</sub> with a Polytron (Brinkmann). The homogenate was then centrifuged at 45,000g for 10 min at 4°C, and the pellet was resuspended in fresh buffer to yield a synaptosomal membrane suspension with a protein concentration of 1 mg/mL.

Binding assays were performed by incubation of 0.1 mL of the cortical synaptosomal membrane suspension (1 mg protein) at 2°C with (-)-<sup>3</sup>H-cytisine (5 nmol/L) and various concentrations of competing drugs in 0.15 mL of 50 mmol/L Tris-HCl buffer (pH 7.4) containing 120 mmol/L NaCl, 5 mmol/L KCl, 1 mmol/L MgCl<sub>2</sub>, and 2.5 mmol/L CaCl<sub>2</sub>. When acetylcholine was used in competition studies, 200 μmol/L diisopropyl fluorophosphate, a cholinesterase inhibitor, was added to the tissue homogenate approximately 30 min before initiation of the assay. Incubation was performed for 75 min at 2°C, after which the samples were rapidly filtered through polylysine-soaked Whatman GF/C filters, and the filters were washed rapidly 3 times with 4 mL of ice-cold assay buffer. Each filter was then placed into a 20-mL scintillation vial containing 10 mL ACS II (Amersham) and the radioactivity bound to the filter was measured with a liquid scintillation counter. The 50% inhibitory concentration (IC<sub>50</sub>) values were determined from displacement curves of the percentage inhibition of (-)-<sup>3</sup>H-cytisine binding versus the inhibitor concentration by means of the LIGAND curve-fitting computer program (Elsevier-Biosoft). For calculation of the inhibition constant (K<sub>i</sub>), the value of 0.96 nmol/L obtained by Pabreza et al. was used as the dissociation constant (K<sub>d</sub>) for (-)-cytisine (30).

### Determination of Brain Uptake Index (BUI)

To assess the permeability of the blood–brain barrier, a BUI study was performed in rats using the double-isotope, intracarotid, single-injection technique of Oldendorf (31). Briefly, a mixture of 200 μL of saline containing <sup>11</sup>C-5MA (3,700 kBq) and <sup>14</sup>C-butanol (37 kBq) was injected into the right common carotid artery of male Wistar rats (250 g), and the rats were killed by decapitation 15 s after the injection. Part of the cortex was removed from each rat and the <sup>11</sup>C radioactivity was measured in a NaI well scintillation counter. After all <sup>11</sup>C had decayed, the samples were treated with NCS tissue solubilizer (Amersham) and the <sup>14</sup>C radioactivity was measured in a liquid scintillation counter. Finally, the BUI was calculated according to the following formula:

$$\text{BUI} = \left( \frac{[^{11}\text{C} \text{ in brain (kBq)}]}{[^{14}\text{C} \text{ in brain (kBq)}]} \right) \times 100.$$

### Biodistribution Studies in Mice

Male ddY mice weighing about 30 g were injected via the tail vein with 3.7 MBq <sup>11</sup>C-5MA in 0.1 mL of saline solution. At the designated times after injection, the mice were killed by decapitation and their organs were removed. Then the tissues were weighed and the radioactivity was measured in a NaI well scintillation counter.

The relative binding affinity of <sup>11</sup>C-5MA for nicotinic acetylcholine receptors was determined with various drugs, which were injected into mice given 3.7 MBq <sup>11</sup>C-5MA. (-)-Cytisine (1 mg/kg), (-)-nicotine (60 μg/kg), dextemide (10 mg/kg), and 5MA (0.1 mg/kg) were injected intravenously 5 min before the radioligand, whereas scopolamine (10 mg/kg) and mecamlamine

(5 mg/kg) were injected subcutaneously 30 min before the radioligand. The mice were killed 30 min after administration of the radioligand; then the brain regions were dissected and the radioactivity was measured in a NaI well scintillation counter.

### Metabolic Studies

Male ddY mice weighing about 30 g were injected intravenously with 111 MBq  $^{11}\text{C}$ -5MA and then decapitated 30 min after injection. The brains were removed immediately and homogenized in 1 mL of methanol. After centrifugation at 1,750g for 5 min at 4°C, the precipitate was washed with 1 mL of methanol and the wash was combined with the supernatant. The combined methanol extracts were evaporated under a stream of nitrogen to a small volume and analyzed by thin-layer chromatography (methanol/10% ammonium acetate aqueous solution, 1:1;  $R_f = 0.43$ –0.50 for  $^{11}\text{C}$ -5MA).

### PET Study of $^{11}\text{C}$ -5MA in Rhesus Monkey

PET studies were performed on a male rhesus monkey (*M. mulatta*), 3.9 kg in body weight, with a multislice PET scanner for animals (SHR-7700; Hamamatsu Photonics K.K.) (32,33). This scanner provided 31 slices of tomographic images at 3.6-mm intervals per frame. Transaxial resolution of the system was 2.6-mm full width at half maximum at the center of the field of view. PET images were reconstructed by the filtered-backprojection method with a Hanning 4.5-mm filter.

After an overnight fast, a monkey was seated in the monkey chair and fixed with stereotactic coordinates aligned parallel to the orbitomeatal line. A cannula was implanted into the posterior tibial vein for administration of a radiolabeled compound. The PET scans were performed under dim light. Eight hundred megabecquerels of  $^{11}\text{C}$ -5MA were injected through the posterior tibial vein cannula. Each PET scan was performed for 121 min with 6 time frames at 10-s intervals, 6 time frames at 30 s, and 12 time frames at 1 min, followed by 35 time frames at 3 min. Regions of interest (ROIs) were identified in 7 cortical regions (frontal, temporal and occipital cortices, striatum, cingulate gyrus, thalamus, and cerebellum) according to MR images, and time-activity curves in ROIs were obtained. Activities in ROIs were calibrated using the cross-calibration factor calculated in the phantom study with a 10-cm-diameter hollow phantom.

In the displacement studies, 5 mg/kg of (–)-cytisine were injected intravenously 90 min before or 50 min after administration of  $^{11}\text{C}$ -5MA (800 MBq). The scanning was performed with the same procedure as in the control study.

### Statistical Analysis

Data are presented as mean  $\pm$  SD. Comparisons between groups were performed with the Dunnett multiple comparisons test.  $P < 0.05$  was considered statistically significant.

## RESULTS

### Radiosynthesis of $^{11}\text{C}$ -5MA

$^{11}\text{C}$ -5MA was synthesized by the incorporation of  $^{11}\text{C}$ -methyl iodide into the stannyl compound using a Pd-catalyzed coupling reaction, followed by deprotection of the *N*-butoxycarbonyl group with acidic condition, referring to the report of Karimi and Langstrom (29) and the report of Suzuki et al. (34); we used the tributylstannyl compound instead of the trimethylstannyl compound as a precursor and

*N,N*-dimethylformamide instead of dimethyl sulfoxide as a solvent (Fig. 1). The tributylstannyl compound has the advantage that it can also be used as a precursor in the synthesis of  $^{123}\text{I}$ -iodinated A-85380 (5IA), a SPECT radiopharmaceutical for nAChRs (21,25,27). The overall synthesis time including the final formulation in saline was 60 min from the end of radionuclide production, and the overall decay-corrected radiochemical yield of  $^{11}\text{C}$ -5MA was 30% calculated from the amount of  $^{11}\text{C}$ -methyl iodide. The radiochemical purity of the product was >99%, with a specific radioactivity of >36 GBq/ $\mu\text{mol}$ , estimated from ultraviolet absorbance at 274 nm.

### In Vitro Binding

Using the reference compounds, A-85380, (–)-cytisine, (–)-nicotine, acetylcholine, mecamylamine, and  $\alpha$ -bungarotoxin, the affinity of 5MA for brain nAChRs was measured by examining competition with (–)- $^3\text{H}$ -cytisine for binding sites in rat cortical membranes. Figure 2 illustrates competitive binding curves representative of these compounds, and the  $K_i$  values determined from  $\text{IC}_{50}$  are summarized in Table 1. 5MA showed approximately 1.5-fold higher affinity than A-85380, 3-fold higher affinity than (–)-cytisine, and 10-fold higher affinity than (–)-nicotine. Since A85380, (–)-cytisine, and (–)-nicotine are compounds with high affinity for central nAChRs (12,18,30), these results indicate that 5MA showed high binding affinity for nAChRs.

### Determination of BUI

The BUI of  $^{11}\text{C}$ -5MA was investigated in rats.  $^{11}\text{C}$ -5MA showed a moderate BUI (mean  $\pm$  SD =  $9.4 \pm 3.1$  with respect to the  $^{14}\text{C}$ -butanol reference).

### Biodistribution Studies in Mice

The results of the radioactivity distribution studies in mice after intravenous administration of  $^{11}\text{C}$ -5MA are summarized in Table 2.  $^{11}\text{C}$ -5MA gradually entered the brain

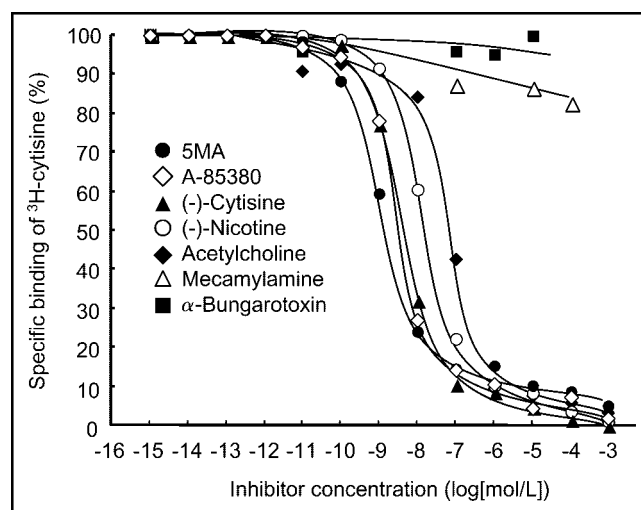


FIGURE 2. Inhibition of (–)- $^3\text{H}$ -cytisine binding to rat cortical membranes by various drugs.

**TABLE 1**  
K<sub>i</sub> Values for Inhibiting (–)-<sup>3</sup>H-Cytisine Binding to Rat Brain Synaptosomal Membranes

Compound	K <sub>i</sub> (nmol/L)
5MA	0.27 ± 0.16*
A-85380	0.38 ± 0.01*
(–)-Cytisine	0.92 ± 0.42*
(–)-Nicotine	2.71 ± 0.73*
Acetylcholine	13.40 ± 2.61*
Mecamylamine	>1,000,000†
α-Bungarotoxin	>1,000,000†

\*Mean ± SD of 3 independent experiments.

†Not inhibited at the highest concentration tested (10<sup>–4</sup> mol/L).

and a high uptake of radioactivity was observed over 15–30 min, after which there was a decline with time. The radioactivity in blood was cleared rapidly. The brain-to-blood ratio of radioactivity increased with time, and the highest ratio was 4.3 at 60 min after injection. A high initial uptake was also observed in the kidneys, pancreas, liver, and lungs, but the radioactivity in these organs cleared rapidly. No abnormality was observed in behavior after injection of <sup>11</sup>C-5MA.

The temporal distribution of the radioactivity in various regions of the mouse brain is shown in Figure 3. Differences in the regional distribution of radioactivity were observed—that is, the thalamus showed the highest uptake, followed by the cortex, striatum, and cerebellum in that order. The thalamus-to-cerebellum ratio gradually increased with time, and the highest value was 2.5 at 60 min. The regional distribution of <sup>11</sup>C-5MA at 30 min parallels the distribution of nAChRs determined by the *in vitro* binding assay (35) (*r* = 0.97) (Fig. 4). Furthermore, the effects of various drugs on the levels of <sup>11</sup>C-5MA in various regions were studied. As shown in Figure 5, the administration of (–)-nicotine

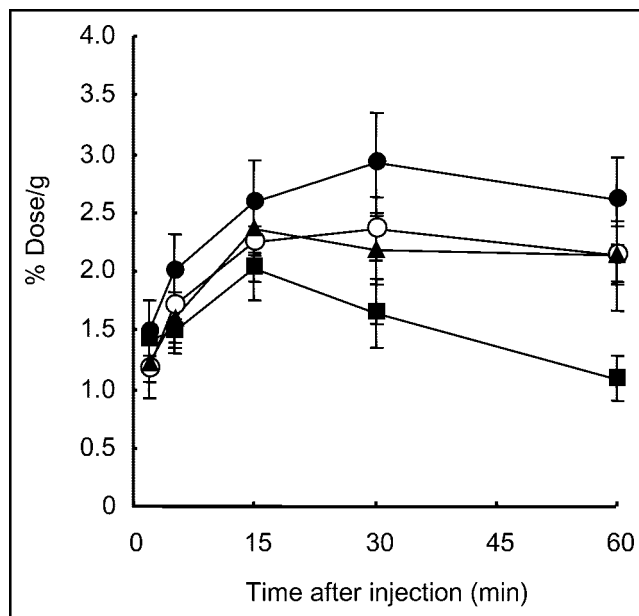


**FIGURE 3.** Regional brain uptake of <sup>11</sup>C-5MA in mice. ●, Thalamus; ○, cortex; ▲, striatum; ■, cerebellum. Data are presented as mean ± SD.

and (–)-cytisine, compounds with high affinity for central nAChRs (13,18,30,36), reduced the uptake of radioactivity at higher magnitude in the region of higher uptake in the untreated brain and resulted in almost the same level throughout the brain. Similar results were observed in the treatment with nonradioactive 5MA. However, the administration of dextimide and scopolamine, drugs with high selective affinity for muscarinic cholinergic receptors (22), caused no changes in the regional uptake. Similar negative results were observed for mice treated with mecamylamine, a noncompetitive nicotinic antagonist (4). None of the compounds tested had an effect on the radioactivity in the blood.

**TABLE 2**  
Biodistribution of Radioactivity After Administration of <sup>11</sup>C-5MA

Biodistribution	Time after injection (min)				
	2	5	15	30	60
Blood	1.73 ± 0.35	1.35 ± 0.02	1.09 ± 0.06	0.83 ± 0.11	0.42 ± 0.02
Intestine	3.08 ± 0.58	3.22 ± 0.56	2.47 ± 0.13	2.44 ± 0.34	1.90 ± 0.39
Liver	7.29 ± 1.30	7.80 ± 0.36	5.53 ± 0.33	4.09 ± 0.52	2.34 ± 0.24
Kidney	20.0 ± 3.99	18.2 ± 0.19	21.6 ± 4.21	6.94 ± 1.09	4.88 ± 0.93
Stomach	2.01 ± 0.17	2.79 ± 0.34	2.56 ± 0.13	3.52 ± 0.52	2.19 ± 1.00
Spleen	3.31 ± 0.68	5.46 ± 0.97	4.28 ± 0.52	4.14 ± 1.83	1.57 ± 0.82
Pancreas	7.77 ± 1.08	7.00 ± 1.23	3.30 ± 0.12	1.93 ± 0.22	0.88 ± 0.24
Heart	4.87 ± 1.60	2.94 ± 0.51	1.53 ± 0.21	1.12 ± 0.30	0.62 ± 0.34
Lung	7.14 ± 2.46	5.78 ± 0.78	2.42 ± 0.46	1.54 ± 0.29	0.94 ± 0.32
Brain	1.23 ± 0.12	1.66 ± 0.09	2.24 ± 0.12	2.19 ± 0.24	1.87 ± 0.21
Br/BI*	0.71 ± 0.15	1.23 ± 0.07	2.06 ± 0.19	2.65 ± 0.23	4.28 ± 0.46

\*Br/BI = brain-to-blood ratio (percentage of injected <sup>11</sup>C dose/gram of organ ratio).

Biodistribution of radioactivity is expressed as percentage of injected <sup>11</sup>C dose/gram of organ (mean ± SD for 4 mice).



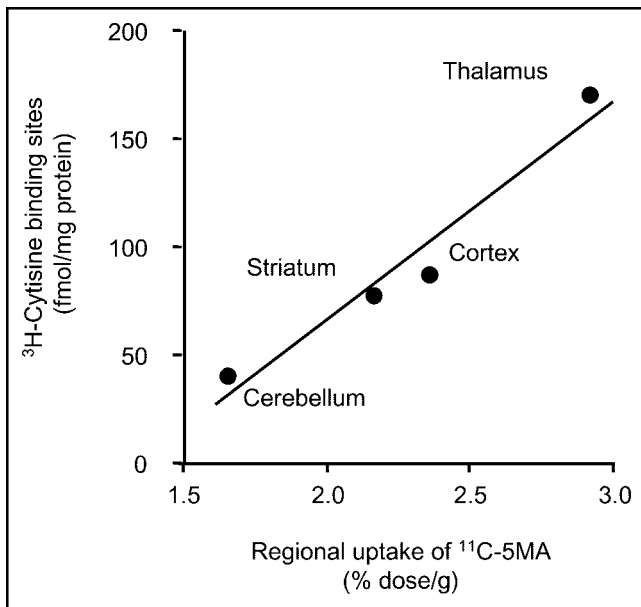


**FIGURE 4.** Correlation between radioactivity levels determined from in vivo distribution of  $^{11}\text{C}$ -5MA and density of nicotinic cholinergic receptor sites as determined by in vitro ( $-$ )- $^3\text{H}$ -cytisine binding (35).

The analysis of brain homogenates was performed at 30 min after injection of  $^{11}\text{C}$ -5MA. Approximately 90% of the radioactivity in the homogenate could be extracted with methanol. No radioactive metabolites were observed in the brain homogenates, indicating that the cerebral accumulation of radioactivity occurred in the intact form.

#### PET Study of $^{11}\text{C}$ -5MA in Rhesus Monkey

A PET imaging study with  $^{11}\text{C}$ -5MA in a rhesus monkey demonstrated high uptake and a noticeably heterogeneous distribution of radioactivity in the brain. Figure 6A shows a PET image of  $^{11}\text{C}$ -5MA in monkey brain slices at 60–90

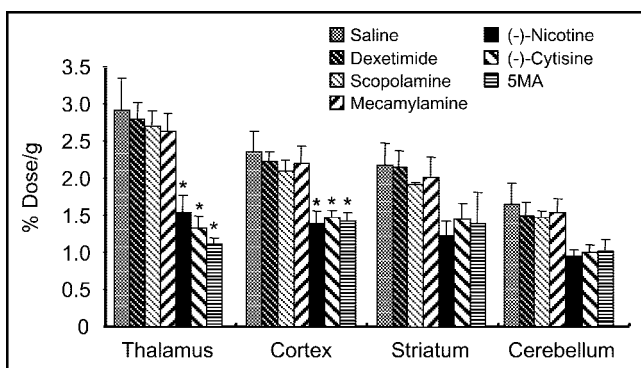


**FIGURE 5.** Effect of various drugs on regional uptake of  $^{11}\text{C}$ -5MA in mice 30 min after injection.  $^{11}\text{C}$ -5MA was intravenously injected 5 min after intravenous administration of ( $-$ )-cytisine (1 mg/kg), ( $-$ )-nicotine (60  $\mu\text{g}/\text{kg}$ ), dextimide (10 mg/kg), 5MA (0.1 mg/kg), and saline and 30 min after subcutaneous administration of scopolamine (10 mg/kg) and mecamylamine (5 mg/kg). Data are presented as mean  $\pm$  SD.  $*P < 0.01$  as compared with saline control group (Dunnett multiple comparisons test).

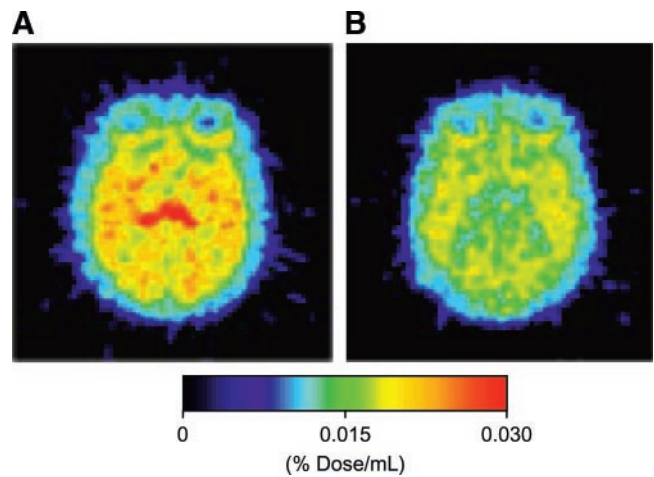


**FIGURE 6.** Transaxial PET images at 60–90 min after injection of  $^{11}\text{C}$ -5MA in rhesus monkey. (A)  $^{11}\text{C}$ -5MA alone. (B) ( $-$ )-Cytisine (5 mg/kg) administered 90 min before  $^{11}\text{C}$ -5MA injection.

min after injection. A high accumulation of radioactivity was observed in the thalamus. Figure 6B shows the effect of ( $-$ )-cytisine on the cerebral distribution of  $^{11}\text{C}$ -5MA. Treatment with ( $-$ )-cytisine 90 min before injection of the radioligand reduced the accumulation of radioactivity in regions of high uptake in the untreated experiment and resulted in nearly identical levels of radioactivity in all regions. Figure 7 shows time–radioactivity curves in the thalamus and cerebellum after intravenous injection of  $^{11}\text{C}$ -5MA. After injection of  $^{11}\text{C}$ -5MA, the radioactivity was rapidly taken up by the brain. Thereafter, the radioactivity in the thalamus increased further with time and then remained constant after 50 min, whereas that in the cerebellum was constant at 5–30 min and then decreased gradually with

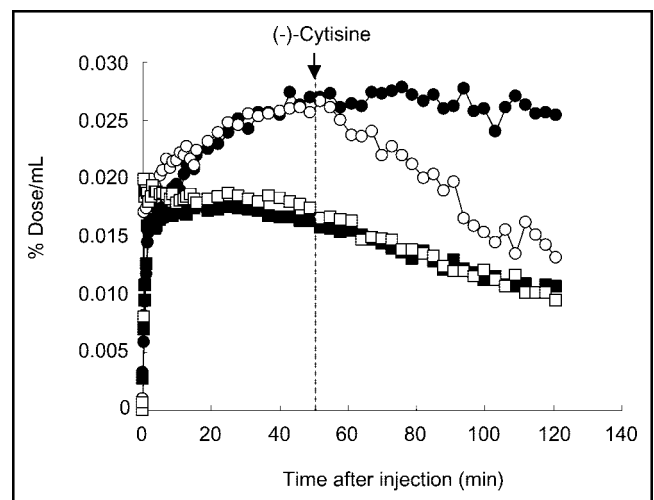


**FIGURE 7.** Time–radioactivity curves of  $^{11}\text{C}$ -5MA in rhesus monkey. ( $-$ )-Cytisine (5.0 mg/kg) was intravenously administered 50 min after  $^{11}\text{C}$ -5MA injection. ●, Thalamus in control study; ■, cerebellum in control study; ○, thalamus in ( $-$ )-cytisine displacement study; □, cerebellum in ( $-$ )-cytisine displacement study.

time after approximately 30 min. The treatment with (–)-cytisine (5 mg/kg, intravenous) 50 min after injection of the radioligand rapidly reduced the radioactivity in the thalamus, resulting in nearly the same level of radioactivity as that in the cerebellum 50 min after (–)-cytisine administration. In contrast, no change in the level of radioactivity was observed in the cerebellum on treatment with (–)-cytisine. The level of radioactivity in the blood was not significantly different after (–)-cytisine treatment.

## DISCUSSION

The basic requirements for the effective use of radioligands for *in vivo* studies of central nAChRs include high affinity and selectivity for the receptors, quantitatively significant brain uptake after peripheral administration, and a regional cerebral distribution that is well correlated with the nAChR density of a site (12).

Since 5IA, an A-85380 analog iodinated at the 5-position of the pyridine ring, showed high affinity for nAChRs without a disturbance of receptor binding (12,21,28,37), it has been suggested that position 5 of the pyridyl fragment is the appropriate site for introduction of the <sup>11</sup>C-methyl group in A-85380. In fact, Holladay et al. recently found that 5MA has high affinity for nAChRs (28). Our study on the receptor-binding assay also confirmed high affinity of 5MA for nAChRs—that is, 5MA has approximately 1.5 times higher affinity than A-85380, 3.5 times higher affinity than (–)-cytisine, and 10 times higher affinity than (–)-nicotine (Fig. 2; Table 1). Thus, the results indicate that position 5 is a suitable site for introduction of the methyl group in the A-85380 molecule.

*In vivo* biodistribution studies with <sup>11</sup>C-5MA showed high accumulation in the brain. The radioactivity in the brain increased with time after injection and the peak level was reached at 15 min, showing an increase by a factor of 1.8 compared with that at 2 min (Table 2). The slightly slow uptake kinetics of <sup>11</sup>C-5MA by the brain may be responsible for the moderate BUI.

Studies on the regional brain distribution showed that 5MA had high accumulation of radioactivity in the thalamus, intermediate accumulation in the cortex, striatum, and hippocampus, and low accumulation in the cerebellum (Fig. 3). This regional distribution correlated well with the known distribution of nAChRs (35) (Fig. 4). In addition, the administration of (–)-cytisine and (–)-nicotine, nAChR-binding agents (13,18,28,30,36), reduced the uptake of radioactivity at higher magnitude in regions of higher uptake in the untreated brain and resulted in almost the same level throughout the brain. However, dextimide, scopolamine, and mecamylamine did not influence the cerebral distribution of <sup>11</sup>C-5MA. These results indicate the selective binding of <sup>11</sup>C-5MA to nAChRs in the brain. Furthermore, injection of nonradioactive 5MA (0.1 mg/kg) resulted in a marked reduction in the uptake of radioactivity in the brain. This finding demonstrated the saturability of the sites la-

beled with <sup>11</sup>C-5MA. These results on selectivity and saturability indicated that <sup>11</sup>C-5MA binds to nAChRs in the brain after intravenous injection.

Imaging studies with PET in rhesus monkey demonstrated that <sup>11</sup>C-5MA can be used to visualize nAChRs in the brain. Furthermore, <sup>11</sup>C-5MA uptake was displaced by treatment with (–)-cytisine, showing that the binding of <sup>11</sup>C-5MA to nAChR sites was reversible.

When the *in vivo* behavior of <sup>11</sup>C-5MA in the mouse brain was compared with previously published data on other A85380 derivatives labeled with a positron radionuclide, 2-<sup>18</sup>F-fluoro-A-85380 (2-<sup>18</sup>F-FA) and 6-<sup>18</sup>F-fluoro-A-85380 (6-<sup>18</sup>F-FA) (38,39), the total uptake and the thalamus-to-cerebellum ratio, target-to-nontarget ratio, of <sup>11</sup>C-5MA in the mouse brain were lower than those of 2-<sup>18</sup>F-FA and 6-<sup>18</sup>F-FA. On the other hand, the uptake rate of <sup>11</sup>C-5MA by the thalamus was comparable with that of 2-<sup>18</sup>F-FA and faster than that of 6-<sup>18</sup>F-FA, and clearance of <sup>11</sup>C-5MA from the thalamus was faster than 6-<sup>18</sup>F-FA and slower than 2-<sup>18</sup>F-FA. However, with regard to the accumulation and clearance in the thalamus, it has been reported that, in the baboon, 6-<sup>18</sup>F-FA exhibited faster accumulation followed by a faster decline compared with that of 2-<sup>18</sup>F-FA, as opposed to the data in mice (40). Thus, although a high uptake and target-to-nontarget ratio of 2-<sup>18</sup>F-FA and 6-<sup>18</sup>F-FA in the mouse brain may be preferable to <sup>11</sup>C-5MA, further comparative studies are required on cerebral behavior of the 3 radioligands in other animals.

In addition, displacement studies of <sup>11</sup>C-5MA showed that some radioactivity remained in the brain after treatment with (–)-nicotine and (–)-cytisine. Although the cause of this finding is unclear, it may be due to high nonspecific binding or a large amount of free ligand in the brain. In this study, the timing of the displacement studies (30 min) may have been too early to remove completely free ligands from the brain because the radioactivity in the cerebellum declined further with time after 30 min (Fig. 3). More studies are required of this high residual uptake.

## CONCLUSION

In this study, <sup>11</sup>C-5MA, an A-85380 derivative <sup>11</sup>C-methylated at position 5 of the pyridyl fragment, was synthesized by rapid <sup>11</sup>C-methylation using <sup>11</sup>C-methyl iodide. *In vitro* competitive binding studies showed high affinity of 5MA for brain nAChRs. *In vivo* biodistribution studies demonstrated that <sup>11</sup>C-5MA showed high brain uptake and regional cerebral distribution in association with nAChRs after intravenous injection. Furthermore, <sup>11</sup>C-5MA allowed visualization of central nAChR sites in the rhesus monkey by PET. Thus, <sup>11</sup>C-5MA is a potential radioligand for use in PET investigations of central nAChRs in humans.

## ACKNOWLEDGMENTS

This work was supported in part by a grant from the Research for the Future Program of the Japan Society for

the Promotion of Science (JSPS-RFTF97K00201); grants-in-aid for Scientific Research from the Ministry of Education, Culture, Sports, Science and Technology of Japan; a grant-in-aid for Creative Scientific Research of the Japan Society for the Promotion of Science; and a grant from the Smoking Research Foundation.

## REFERENCES

- Irle E, Markowitsch HJ. Basal forebrain-lesioned monkeys are severely impaired in tasks of association and recognition memory. *Ann Neurol*. 1987;22:735–743.
- Decker MW, Brioni JD, Bannon AW, Americ SP. Diversity of neuronal nicotinic acetylcholine receptors: lessons from behavior and implications for CNS therapeutics. *Life Sci*. 1995;56:545–570.
- White HK, Levin ED. Four-week nicotine skin patch treatment effects on cognitive performance in Alzheimer's disease. *Psychopharmacology (Berl)*. 1999;143:158–165.
- Paterson D, Nordberg A. Neuronal nicotinic receptors in the human brain. *Prog Neurobiol*. 2000;61:75–111.
- Nordberg A, Alafuzoff I, Winblad B. Nicotinic and muscarinic subtypes in the human brain: changes with aging and dementia. *J Neurosci Res*. 1992;31:103–111.
- Flynn DD, Mash DC. Characterization of L-[<sup>3</sup>H]nicotine binding in human cerebral cortex: comparison between Alzheimer's disease and the normal. *J Neurochem*. 1986;47:1948–1954.
- London ED, Ball MJ, Waller SB. Nicotinic binding sites in cerebral cortex and hippocampus in Alzheimer's dementia. *Neurochem Res*. 1989;14:745–750.
- Sihver W, Gillberg PG, Svensson AL, Nordberg A. Autoradiographic comparison of [<sup>3</sup>H](–)nicotine, [<sup>3</sup>H]cytisine and [<sup>3</sup>H]epibatidine binding in relation to vesicular acetylcholine transport sites in the temporal cortex in Alzheimer's disease. *Neuroscience*. 1999;94:685–696.
- Whitehouse PJ, Martino AM, Wagster MV, et al. Reductions in [<sup>3</sup>H]nicotinic acetylcholine binding in Alzheimer's disease and Parkinson's disease: an autoradiographic study. *Neurology*. 1988;38:720–723.
- Perry EK, Morris CM, Court JA, et al. Alteration in nicotine binding sites in Parkinson's disease, Lewy body dementia and Alzheimer's disease: possible index of early neuropathology. *Neuroscience*. 1995;64:385–395.
- Perry DC, Davila-Garcia MI, Stockmeier CA, Kellar KJ. Increased nicotinic receptors in brains from smokers: membrane binding and autoradiography studies. *J Pharmacol Exp Ther*. 1999;289:1545–1552.
- Sihver W, Nordberg A, Langstrom B, et al. Development of ligands for *in vivo* imaging of cerebral nicotinic receptors. *Behav Brain Res*. 2000;113:143–157.
- Nyback H, Halldin C, Ahlin A, et al. PET studies of the uptake of (S)- and (R)-[<sup>11</sup>C]nicotine in the human brain: difficulties in visualizing specific receptor binding *in vivo*. *Psychopharmacology (Berl)*. 1994;115:31–36.
- Saji H, Watanabe A, Magata Y, et al. Synthesis and characterization of radioiodinated (S)-5-iodonicotine: a new ligand for potential imaging of brain nicotinic cholinergic receptors by single photon emission computed tomography. *Chem Pharm Bull*. 1997;45:284–290.
- Horti A, Scheffel U, Stathis M, et al. Fluorine-18-FPH for PET imaging of nicotinic acetylcholine receptors. *J Nucl Med*. 1997;38:1260–1265.
- Ding YS, Molina PE, Fowler JS, et al. Comparative studies of epibatidine derivatives [<sup>18</sup>F]NFEP and [<sup>18</sup>F]N-methyl-NFEP: kinetics, nicotine effect, and toxicity. *Nucl Med Biol*. 1999;26:139–148.
- Sullivan JP, Donnelly-Roberts D, Briggs CA, et al. A-85380 [3-(2(S)-azetidylmethoxy)pyridine]: *in vitro* pharmacological properties of a novel, high affinity alpha 4 beta 2 nicotinic acetylcholine receptor ligand. *Neuropharmacology*. 1996;35:725–734.
- Abreo MA, Lin NH, Garvey DS, et al. Novel 3-pyridyl ethers with subnanomolar affinity for central neuronal nicotinic acetylcholine receptors. *J Med Chem*. 1996;39:817–825.
- Valette H, Bottlaender M, Dolle F, et al. Imaging central nicotinic acetylcholine receptors in baboons with [<sup>18</sup>F]fluoro-A-85380. *J Nucl Med*. 1999;40:1374–1380.
- Horti AG, Chefer SI, Mukhin AG, et al. 6-[<sup>18</sup>F]Fluoro-A-85380, a novel radioligand for *in vivo* imaging of central nicotinic acetylcholine receptors. *Life Sci*. 2000;67:463–469.
- Koren AO, Horti AG, Mukhin AG, et al. 2-, 5-, and 6-Halo-3-(2(S)-azetidylmethoxy)pyridines: synthesis, affinity for nicotinic acetylcholine receptors, and molecular modeling. *J Med Chem*. 1998;41:3690–3698.
- Vaupel DB, Mukhin AG, Kimes AS, Horti AG, Koren AO, London ED. *In vivo* studies with [<sup>125</sup>I]-5-I-A-85380, a nicotinic acetylcholine receptor radioligand. *Neuroreport*. 1998;9:2311–2317.
- Musachio JL, Scaffel U, Finley PA, et al. 5-[I-125/123]Iodo-3(2(S)-azetidylmethoxy)pyridine, a radioiodinated analog of A-85380 for *in vivo* studies of central nicotinic acetylcholine receptors. *Life Sci*. 1998;62:351–357.
- Chefer SI, Horti AG, Lee KS, et al. *In vivo* imaging of brain nicotinic acetylcholine receptors with 5-[<sup>123</sup>I]iodo-A-85380 using single photon emission computed tomography. *Life Sci*. 1998;63:355–360.
- Musachio JL, Villemagne VL, Scaffel UA, et al. Synthesis of an I-123 analog of A-85380 and preliminary SPECT imaging of nicotinic receptors in baboon. *Nucl Med Biol*. 1999;26:201–207.
- Fujita M, Tamagnan G, Zoghbi SS, et al. Measurement of  $\alpha_4\beta_2$  nicotinic acetylcholine receptors with [I-123]5-I-A-85380 SPECT. *J Nucl Med*. 2000;41:1552–1560.
- Saji H, Ogawa M, Ueda M, et al. Evaluation of radioiodinated 5-iodo-3-(2(S)-azetidylmethoxy)pyridine as a ligand for SPECT investigations of brain nicotinic acetylcholine receptors. *Ann Nucl Med*. 2002;16:189–200.
- Holladay MW, Bai H, Li Y, et al. Structure-activity studies related to ABT-594, a potent nonopioid analgesic agent: effect of pyridine and azetidine ring substitutions on nicotinic acetylcholine receptor binding affinity and analgesic activity in mice. *Bioorg Med Chem Lett*. 1998;8:2797–2802.
- Karimi F, Langstrom B. Synthesis of 3-[(2S)-azetidyl-2-ylmethoxy]-5-[<sup>11</sup>C]-methylpyridine, an analogue of A-85380, via a Still coupling. *J Labelled Compd Radiopharm*. 2002;45:423–434.
- Pabreza LA, Dhawan S, Kellar KJ. [<sup>3</sup>H]Cytisine binding to nicotinic cholinergic receptors in brain. *Mol Pharmacol*. 1991;39:9–12.
- Oldendorf WH. Measurement of brain uptake of radiolabeled substances using a tritiated water internal standard. *Brain Res*. 1970;24:372–376.
- Magata Y, Saji H, Choi SR, et al. Noninvasive measurement of cerebral blood flow and glucose metabolic rate in the rat with high-resolution animal positron emission tomography (PET): a novel *in vivo* approach for assessing drug action in the brains of small animals. *Biol Pharm Bull*. 1995;18:753–756.
- Tsukada H, Harada N, Nishiyama S, et al. Ketamine decreased striatal [<sup>11</sup>C]raclopride binding with no alterations in static dopamine concentrations in the striatal extracellular fluid in the monkey brain: multiparametric PET studies combined with microdialysis analysis. *Synapse*. 2000;37:95–103.
- Suzuki M, Doi H, Björkman M, et al. Rapid coupling of methyl iodide with aryltributylstannanes mediated by palladium(0) complexes: a general protocol for the synthesis of <sup>11</sup>C-labeled PET tracers. *Chem Eur J*. 1997;3:2039–2041.
- Sargent PB. The diversity of neuronal nicotinic acetylcholine receptors. *Annu Rev Neurosci*. 1993;16:403–443.
- Flesher JE, Scheffel U, London ED, Frost JJ. *In vivo* labeling of nicotinic cholinergic receptors in the brain with [<sup>3</sup>H]cytisine. *Life Sci*. 1994;54:1883–1890.
- Mukhin AG, Gundisch D, Horti AG, et al. 5-Iodo-A-85380, an  $\alpha_4\beta_2$  subtype-selective ligand for nicotinic acetylcholine receptors. *Mol Pharmacol*. 2000;57:642–649.
- Horti AG, Scheffel U, Koren AO, et al. 2-[<sup>18</sup>F]Fluoro-A-85380, an *in vivo* tracer for the nicotinic acetylcholine receptors. *Nucl Med Biol*. 1998;25:599–603.
- Scheffel U, Horti AG, Koren AO, et al. 6-[<sup>18</sup>F]Fluoro-A-85380: an *in vivo* tracer for the nicotinic acetylcholine receptors. *Nucl Med Biol*. 2000;27:51–56.
- Ding YS, Wang T, Marecek J, et al. Synthesis and evaluation of 6-[<sup>18</sup>F]fluoro-3-(2(S)-azetidylmethoxy)pyridine as a PET tracer for nicotinic acetylcholine receptors. *Nucl Med Biol*. 2000;27:381–389.